Wilson, P.A., Lyle, M., and Firth, J.V. (Eds.)
Proceedings of the Ocean Drilling Program, Scientific Results Volume 199

23. Biogenic Burial across the Paleocene/Eocene Boundary: Ocean Drilling Program Leg 199 Site 1221[1]

Brandi Murphy,[2] Mitchell Lyle,[2] and Annette Olivarez Lyle[2]

ABSTRACT

The Paleocene/Eocene (P/E) boundary, at ~55 Ma, is characterized by a transient warm period lasting 10,000 yr. This interval is globally characterized by significant chemical and biological signals. Ocean Drilling Program Core 199-1221C-11X captured the P/E boundary section at a depth of 154 meters composite depth. Biogenic components of the sediment were measured across this interval in order to better define the events that occurred at the P/E boundary in the equatorial Pacific Ocean. A 26-cm interval low in $CaCO_3$ was identified, whereas biogenic silica and organic carbon remained unchanged. Although $CaCO_3$, biogenic silica, and organic carbon (C-org) production is controlled by different constraints, it is unlikely that an environmental factor would cease production by $CaCO_3$-producing organisms without affecting biogenic silica or C-org production. The data indicate that the $CaCO_3$ P/E boundary event was caused by a change in $CaCO_3$ preservation rather than a change in $CaCO_3$ production.

INTRODUCTION

The Paleocene/Eocene (P/E) boundary, sometimes referred to as the Paleocene/Eocene Thermal Maximum, at ~55 Ma, was a warm period in the Earth's history marked by several unusual excursions recorded in marine sediments. Oxygen isotopes ($\delta^{18}O$) and carbon isotopes ($\delta^{13}C$) at this boundary dropped 2‰–3‰ in <10,000 yr, implying a warming of

[1]Murphy, B., Lyle, M., and Olivarez Lyle, A., 2006. Biogenic burial across the Paleocene/Eocene boundary: Ocean Drilling Program Leg 199 Site 1221. *In* Wilson, P.A., Lyle, M., and Firth, J.V. (Eds.), *Proc. ODP, Sci. Results,* 199, 1–12 [Online]. Available from World Wide Web: <http://www-odp.tamu.edu/publications/199_SR/VOLUME/CHAPTERS/215.PDF>. [Cited YYYY-MM-DD]
[2]Center for the Geophysical Investigation of the Shallow Subsurface, Boise State University, MG206, 1910 University Drive, Boise ID 83725, USA. Correspondence author:
murphyb@ucsd.edu

Initial receipt: 19 April 2004
Acceptance: 24 October 2005
Web publication: 16 June 2006
Ms 199SR-215

bottom waters by 4°–8°C and a significant change in the carbon cycle (Kennett and Stott, 1991; Bralower et al., 1995; Thomas and Shackleton, 1996; Schmitz et al., 1996).

The initiation of the P/E boundary event is marked by the extinction of 35%–50% of cosmopolitan benthic foraminifers, the largest extinction in the Cenozoic (Thomas and Shackleton, 1996; Norris and Röhl, 1999; Katz et al., 1999). The benthic extinction event that defines the P/E boundary is found at Site 1221 (Section 199-1221C-11X-3, 91 cm) (Lyle, Wilson, Janecek, et al., 2002).

The P/E boundary is characterized by a sediment interval low in $CaCO_3$. Calcium carbonate concentration as low as 10 wt% in sections recovered from Ocean Drilling Program (ODP) Legs 171, 189, and 198. Typical $CaCO_3$ concentrations, ranging 1.5–10.0 wt%, were found at all Leg 199 sites where the P/E boundary was recovered (Lyle, Wilson, Janecek, et al., 2002).

METHODS

All carbon and silica analyses were conducted at Boise State University (BSU; Idaho, USA). Opal procedures followed Olivarez Lyle and Lyle (2002), who modified the methods of Mortlock and Froelich (1989) to address the problem of dissolution-resistant Eocene radiolarians. Biogenic opal is a hydrated form of silica sometimes averaging up to 10%–15% water. No corrections were made for water in the crystalline structure, and for this reason, data are reported as biogenic silica without any assumptions of water content. Carbon procedures followed Lyle et al. (2000). A second acidification was applied to samples enriched in calcium carbonate or dolomite. Before analysis, all samples were first freeze-dried, ground with mortar and pestle, and stored in glass vials placed in desiccant to prevent equilibration with ambient moisture.

To assess precision and accuracy, both silica and carbon analyses are performed with in-house standards included in each run. Two opal standards were included with silica analyses: a composite standard containing sediments from ODP Cores 199-1219A-19H through 22H, prepared at BSU, and a standard supplied by Steve Hovan at Indiana University of Pennsylvania (USA), a radiolarian ooze composite containing samples from several Hole 1219A core catchers. Analyses of Hovan's standard averaged 65.8 ± 4.4 wt% silica (N = 45) (Table T1). The BSU composite standard averaged 56.3 ± 1.7 wt% silica (N = 52). Carbon analysis is conducted with a "Midway" standard from the Multitracer site in the northeast Pacific, W8709A-5BC: 5–20 cm. The Midway standard averaged 2.64 ± 0.02 wt% total carbon (N = 523). Organic carbon (C-org) in the same standard averaged 0.85 ± 0.01 wt% (N = 570).

T1. Biogenic components, p. 10.

BIOGENIC COMPONENTS

Calcium carbonate is the dominant component making up 80–90 wt% of the sediment for the majority of the core; however, across the P/E boundary silica dominates at ~30 wt% of the sediment (Fig. F1). Organic carbon consistently remains below 0.25 wt%. To remove the effect of dilution by $CaCO_3$, carbonate-free (CC-free) values were calculated using the equation below, where "A" represents the concentration of biogenic silica or C-org:

F1. Profiles of $CaCO_3$, C-org, and opal, p. 8.

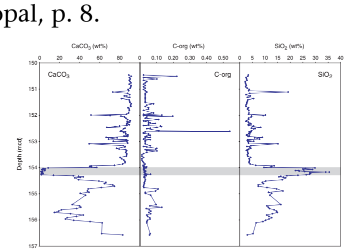

$$A_{CC\text{-}free} = A_{meas} \times (100/100 - CaCO_3)$$

Silica shows no change across the P/E boundary, implying that the measured increase is a lack of $CaCO_3$ dilution rather than a change in silica production or preservation (Fig. F2).

F2. Profiles of C-org and opal, p. 9.

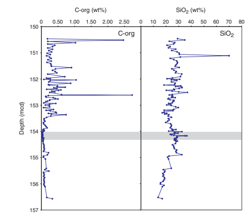

There is a discrepancy between the highest measured opal content vs. the amount of opal that could be visually observed in smear slides (Shipboard Scientific Party, 2002). The highest opal values obtained from the dissolution method were not supported by visual inspection of the sediment in smear slides; obvious radiolarian or other biogenic silica fragments were not seen in "high-opal" intervals. This was true even after the sediments were precleaned with acid to remove calcium carbonate. Biogenic silica fragments are either highly corroded and/or very small, or the samples contain some other soluble nonbiogenic component such as volcanic ash or glass. Previous work has demonstrated that our dissolution technique does not result in SiO_2 contamination by aluminosilicate clay minerals but does dissolve volcanic ash (Olivarez Lyle and Lyle, 2002). Zeolites were identified in this section (Shipboard Scientific Party, 2002), but a test of the solubility of a pure phase of this component has not been done. However, experimental studies of zeolites show that they can crystallize very quickly (2–6 hr) under very high pH conditions (between ~11 and 13.8 pH) and at temperatures of 105°C (Lechert, 2001). These conditions are comparable to those of our analytical method for Leg 199 samples (85°C for 9 hr; pH = ~13), indicating that the zeolites in our samples are not a source of excess silica contributing to the biogenic silica measurements but may be consuming biogenic silica. Regarding volcanic glass, there is one relevant smear slide (Sample 199-1221C-11X-3, 75–78 cm) (Shipboard Scientific Party, 2002) in which a small amount was identified: in this case, ~5%. Olivarez Lyle and Lyle (2002) showed that volcanic glass or ash will readily dissolve during the wet-digestion method for the solvents, sodium carbonate, and potassium hydroxide, thus overestimating the amount of biogenic silica. Our problem, therefore, is to estimate how the presence of glass, identified in one sample, affected our reported biogenic silica values.

The approach used is based on the observation by Olivarez Lyle and Lyle (2002) that the residue of a marine volcanic sedimentary ash layer, recovered after an initial digestion in KOH, will readily dissolve again to near-saturation concentrations when subjected to a second digestion. That is, to a first approximation, the weight percent SiO_2 measured for the second digestion is the same as that measured for the first digestion when volcanic ash is in excess. If samples from Hole 1221C contain significant amounts of volcanic glass, a second digestion of the sediment residue would produce SiO_2 values of the same magnitude as the first analysis. On the other hand, if there is little or no volcanic glass in the recovered residue, then after the second digestion the amount of measured SiO_2 is expected to be very low. To test this hypothesis, eight of the most suspect samples were reanalyzed in replicate. This group included a sample from the identical interval containing ~5% volcanic glass (Sample 199-1221C-11X-3, 76–77 cm), as well as five additional samples taken above and below this glass-bearing interval. The remaining two samples were from the anomalous opal "spike" section at 151.105 meters composite depth (mcd) (Samples 199-1221C-11X-1, 70–71 cm, and 11X-1, 75–76 cm). This interval was suspect because the biogenic silica values were very high relative to those from surrounding samples (20 vs. 4 wt%).

The results of this test indicate there was little to no volcanic glass present in the sediment residue for samples at 151.105 mcd (0.4 wt% SiO_2 for the residue vs. 19 wt% for the first dissolution of the sediment). For the lower interval, Sample 199-1221C-11X-3, 64–83 cm (154.045–154.225 mcd), a small amount of volcanic glass may have survived the first digestion; the average amount of "biogenic silica" measured in the residues was ~3 wt%, in contrast to an average of ~30 wt% SiO_2 for the first dissolution. The independent estimate (from smear slide) of volcanic glass is ~5%; as such, the reported biogenic silica values are likely too high by this amount. Therefore, overall impact of glass contamination for the interval between 154.035 and 154.235 should be minor because, even when corrected for ~5 wt% glass, the data remain relatively unchanged.

Organic carbon measurements at 150.505 and 152.605 mcd remain high after dilution by $CaCO_3$. Since C-org is isolated by dissolution of the bulk sample with a dilute acid, high C-org values may indicate an incomplete dissolution of a resistant carbonate-like dolomite. In order to rule out the presence of dolomite, several samples with relatively higher organic carbon values were remeasured after increasing the amount of acid used to acidify the samples. The samples were acidified three times using 15 drops of 10% HCl, with little observed change in the results. Dolomite contamination, therefore, likely did not cause the high organic carbon measurements.

DISCUSSION

The P/E boundary interval exhibits drastic changes in $CaCO_3$ content, dropping from 80 wt% down to 10 wt% and rising back up again in a 26-cm interval. At the same time, there is no change in biogenic silica or C-org contents. Although there is the possibility of volcanic glass present in the P/E boundary interval, the largest estimates are only ~5%. Even when corrected for 5% glass, the data indicate that there was no change in biogenic silica production across the P/E boundary. Several C-org peaks are present in Section 199-1221C-11X-3. Whereas two of these may be a product of incomplete dissolution of $CaCO_3$, the rest seem to indicate increased C-org preservation, production, or other source. Evidence supporting contamination is the organic geochemical analysis result of Sample 199-1221C-11X-2, 10–12 cm (**Lyle et al.,** this volume), which had 0.66 wt% C-org but only contaminant biomarkers. The issue of high organic carbon spikes is also discussed in **Olivarez Lyle and Lyle** (this volume), although their elevated C-org levels are not within the P/E boundary interval.

Calcium carbonate and biogenic silica content in marine sediment is controlled by variable rates of production and dissolution; however, if $CaCO_3$ production decreased by 70% it would not be unreasonable to expect a decrease in biogenic silica values as well. This is not the case; the raw data show an increase in biogenic silica. When considering the dilution effect of $CaCO_3$, biogenic silica experiences no change before, during, or after the P/E low carbonate event. Dissolution of $CaCO_3$ up to 30 cm is an expected result of methane hydrate dissociation (Dickens et al., 1995), suggesting that a change in preservation of $CaCO_3$ occurred, rather than a change in $CaCO_3$ production.

There is very little evidence for anoxia in the P/E boundary interval. The C-org content remains constant before, during, and after the P/E boundary interval. High levels of manganese oxides found in Hole

1221C sediments from the P/E boundary interval (Shipboard Scientific Party, 2002) are inconsistent with an anoxic environment because this would favor the dissolution of manganese (Stumm and Morgan, 1981). Typically, high manganese in sediments marks the base of a mild redox interval, a result of moving through the sediments beneath oxygenated water and referred to as suboxic diagenesis (Froelich et al., 1979). Changes in redox gradients can leave relict manganese oxide peaks in the sediments (Finney et al., 1988).

An increase in barium (Ba^{2+}; from smear slides) at the P/E boundary interval supports the idea that this was a time of increased productivity as suggested by Bains et al. (2000). However, large amounts of Ba^{2+} may not indicate increased production, per se, because alternate sources are possible. For example, dissolved Ba^{2+} is present in areas with methane hydrates, and methane hydrate dissociation would result in Ba^{2+} fronts within the sediment column (Dickens, 2001).

CONCLUSIONS

Whereas preliminary Ba^{2+} data suggest that the P/E boundary is characterized by elevated productivity, a $CaCO_3$ hiatus would argue just the opposite: a decrease in productivity. At the same time, biogenic silica and C-org data reflect no change in productivity at Site 1221 at the P/E boundary. The three conflicting arguments might be resolved by accounting for a methane hydrate release as suggested by Dickens et al. (1995). Based upon biogenic silica and C-org data, productivity did not decline or increase at the P/E boundary. Oxidation of methane could have resulted in dissolution of $CaCO_3$, while hydrate dissociation released dissolved Ba^{2+}.

Site 1221 was not anoxic at the P/E boundary, as there was no increase in C-org. Although C-org can degrade in anoxic environments, the presence of high Mn^{2+} suggests that this was not the case.

ACKNOWLEDGMENTS

This research used samples and/or data provided by the Ocean Drilling Program (ODP). ODP is sponsored by the U.S. National Science Foundation (NSF) and participating countries under management of Joint Oceanographic Institutions (JOI), Inc. Funding for this research was provided by U.S. Science Support Program and NSF grant OCE-0240906. Carbon analysis performed by Linda Kenoyer and Brandi Murphy. Opal analysis performed by Brandi Murphy.

REFERENCES

Bains, S., Norris, R.D., Corfield, R.M., and Faul, K.L., 2000. Termination of global warmth at the Palaeocene–Eocene boundary through productivity feedback. *Nature (London, U. K.),* 407:171–174.

Bralower, T.J., Zachos, J.C., Thomas, E., Parrow, M., Paull, C.K., Kelly, D.C., Premoli Silva, I., Sliter, W.V., and Lohmann, K.C., 1995. Late Paleocene to Eocene paleoceanography of the equatorial Pacific Ocean: stable isotopes recorded at Ocean Drilling Program Site 865, Allison Guyot. *Paleoceanography,* 10(40):841–865.

Dickens, G.R., 2001. Sulfate profiles and barium fronts in sediment on the Blake Ridge: present and past methane fluxes through a large gas hydrate reservoir. *Geochim. Cosmochim. Acta,* 65:529–543.

Dickens, G.R., O'Neil, J.R., Rea, D.K., and Owen, R.M., 1995. Dissociation of oceanic methane hydrate as a cause of the carbon isotope excursion at the end of the Paleocene. *Paleoceanography,* 10:965–971.

Finney, B.P., Lyle, M.W., and Heath, G.R., 1988. Sedimentation at MANOP Site H (eastern equatorial Pacific) over the past 400,000 years: climatically induced redox variations and their effects on transition metal cycling. *Paleoceanography,* 3:169–189.

Froelich, P.N., Klinkhammer, G.P., Bender, M.L., Luedtke, N.A., Heath, G.R., Cullen, D., Dauphin, P., Hammond, D., Hartman, B., and Maynard, V., 1979. Early oxidation of organic matter in pelagic sediments of the eastern equatorial Atlantic: suboxic diagenesis. *Geochim. Cosmochim. Acta,* 43:1075–1090.

Katz, M.E., Pak, D.K., Dickens, G.R., and Miller, K.G., 1999. The source and fate of massive carbon input during the latest Paleocene thermal maximum. *Science,* 286:1531–1533.

Kennett, J.P., and Stott, L.D., 1991. Abrupt deep-sea warming, paleoceanographic changes and benthic extinctions at the end of the Palaeocene. *Nature (London, U. K.),* 353:225–229.

Lechert, H., 2001. The pH-value and its importance for the crystallization of zeolites. *In* Robson, H. (Ed.), *Verified Syntheses of Zeolitic Materials* (2nd ed.). Available from World Wide Web: <**http://www.iza-synthesis.org/IZA_Publications.htm**>. [Cited 2004-04-16]

Lyle, M., Mix, A., Ravelo, A.C., Andreasen, D.H., Heusser, L.E., and Olivarez, A., 2000. Millennial-scale $CaCO_3$ and C_{org} events along the northern and central California margins: stratigraphy and origins. *In* Lyle, M., Koizumi, I., Richter, C., and Moore, T.C. (Eds.), *Proc. ODP, Sci. Results,* 167, 163–182 [Online]. Available from World Wide Web: <**http://www-odp.tamu.edu/publications/167_SR/chap_11/chap_11.htm**>. [Cited 2003-05-12]

Lyle, M., Wilson, P.A., Janecek, T.R., et al., 2002. *Proc. ODP, Init. Repts.,* 199 [Online]. Available from World Wide Web: <**http://www-odp.tamu.edu/publications/199_IR/199ir.htm**>. [Cited 2003-05-12]

Mortlock, R.A., and Froelich, P.N., 1989. A simple method for the rapid determination of biogenic opal in pelagic marine sediments. *Deep-Sea Res., Part A,* 36:1415–1426.

Norris, R.D., and Röhl, U., 1999. Carbon cycling and chronology of climate warming during the Palaeocene/Eocene transition. *Nature (London, U. K.),* 401:775–778.

Olivarez Lyle, A., and Lyle, M.W., 2002. Determination of biogenic opal in pelagic marine sediments: a simple method revisited. *In* Lyle, M., Wilson, P.A., Janecek, T.R., et al., *Proc. ODP, Init. Repts.,* 199 [Online]. Available from World Wide Web: <**http://www-odp.tamu.edu/publications/199_IR/chap_06/chap_06.htm**>. [Cited 2003-05-12]

Schmitz, B., Speijer, R.P., and Aubry, M.-P., 1996. Latest Paleocene benthic extinction event on the southern Tethyan shelf (Egypt): foraminiferal stable isotopic ($\delta^{13}C$, $\delta^{18}O$) records. *Geology,* 24:347–350.

Shipboard Scientific Party, 2002. Leg 199 Preliminary Report. *ODP Prelim. Rpt.,* 199 [Online]. Available from World Wide Web: <**http://www-odp.tamu.edu/publications/prelim/199_prel/199PREL.PDF**>. [Cited 2004-04-16]

Stumm, W., and Morgan, J.J., 1981. *Aquatic Chemistry* (2nd ed.): New York (Wiley).

Thomas, E., and Shackleton, N., 1996. The Palaeocene–Eocene benthic foraminiferal extinction and stable isotope anomalies. *In* Knox, R.W.O'B., Corfield, R.M., and Dunay, R.E. (Eds.), *Correlation of the Early Paleogene in Northwest Europe.* Geol. Soc. Spec. Publ., 101:401–441.

Figure F1. Profiles of $CaCO_3$, C-org, and opal with depth. Opal values are not corrected for structural water.

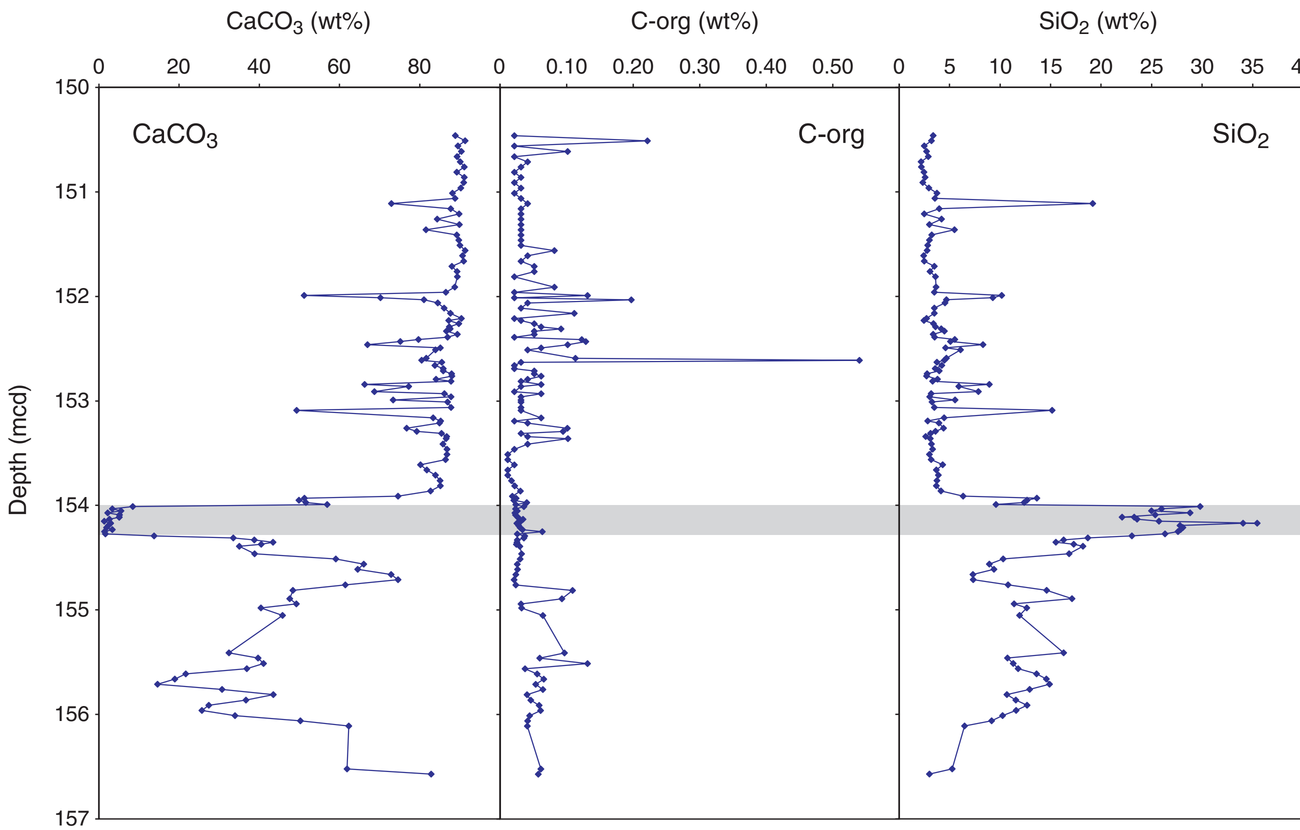

Figure F2. Profiles of C-org and opal adjusted for the dissolution of $CaCO_3$.

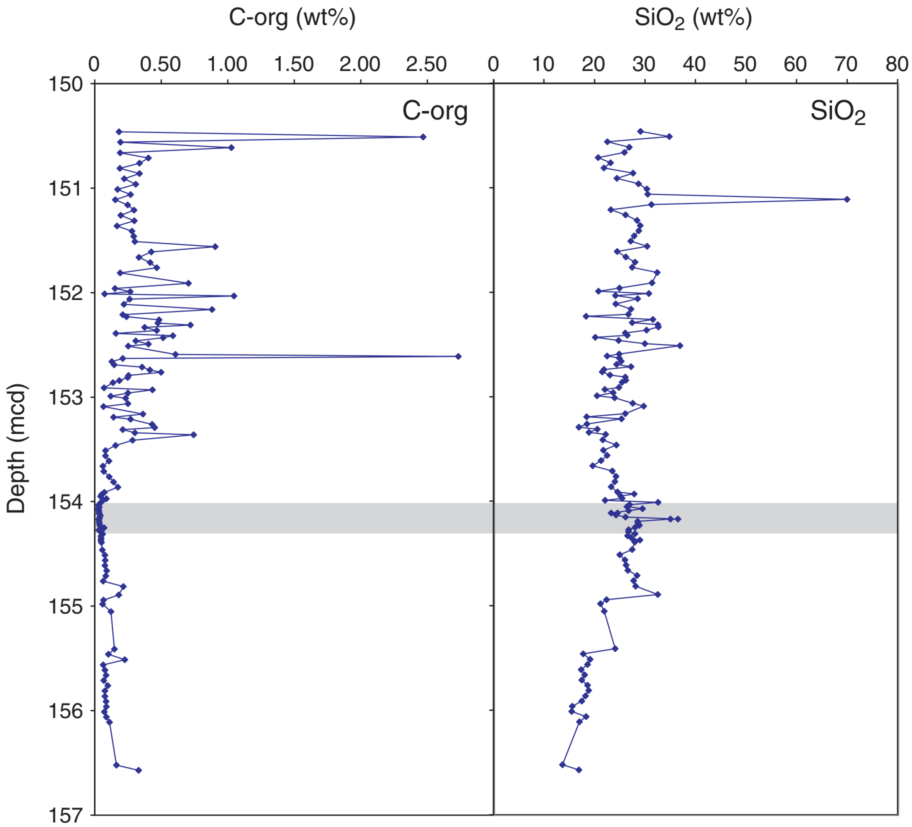

Table T1. Biogenic components, Hole 1221C. (**See table notes.** Continued on next two pages.)

Core, section, interval (cm)	Average mcd	Average carbon (wt%)				Average SiO_2 (wt%)	Carbonate-free elements (wt%)	
		Total	Inorganic	Organic	$CaCO_3$		SiO_2	Organic carbon
199-1221C-								
11X-1, 5–6	150.455	10.66	10.64	0.02	88.66	3.28	28.90	0.18
11X-1, 10–11	150.505	11.15	10.93	0.22	91.06	3.09	34.61	2.46
11X-1, 15–16	150.555	10.74	10.72	0.02	89.31	2.39	22.35	0.19
11X-1, 20–21	150.605	10.93	10.82	0.10	90.19	2.62	26.71	1.02
11X-1, 25–26	150.655	10.71	10.69	0.02	89.11	2.80	25.71	0.18
11X-1, 30–31	150.705	10.82	10.79	0.04	89.88	2.08	20.55	0.40
11X-1, 35–36	150.755	10.93	10.90	0.03	90.87	2.10	23.00	0.33
11X-1, 40–41	150.805	10.70	10.68	0.02	89.04	2.37	21.65	0.18
11X-1, 45–46	150.855	10.94	10.91	0.03	90.91	2.49	27.43	0.33
11X-1, 50–51	150.905	10.91	10.88	0.02	90.71	2.25	24.23	0.22
11X-1, 55–56	150.955	10.83	10.80	0.03	90.01	2.85	28.52	0.30
11X-1, 60–61	151.005	10.57	10.55	0.02	87.91	3.65	30.15	0.17
11X-1, 65–66	151.055	10.66	10.63	0.03	88.58	3.46	30.33	0.26
11X-1, 70–71	151.105	8.76	8.72	0.04	72.67	19.08	69.80	0.15
11X-1, 75–76	151.155	10.53	10.50	0.03	87.51	3.88	31.10	0.24
11X-1, 80–81	151.205	10.78	10.75	0.03	89.57	2.40	23.01	0.29
11X-1, 85–86	151.255	10.13	10.10	0.03	84.15	4.11	25.96	0.19
11X-1, 90–91	151.305	10.80	10.76	0.03	89.68	2.91	28.23	0.29
11X-1, 95–96	151.355	9.79	9.76	0.03	81.35	5.38	28.86	0.16
11X-1, 100–101	151.405	10.72	10.68	0.03	89.03	3.13	28.56	0.27
11X-1, 105–106	151.455	10.77	10.74	0.03	89.52	2.90	27.67	0.29
11X-1, 110–111	151.505	10.81	10.78	0.03	89.83	2.74	26.96	0.29
11X-1, 115–116	151.555	11.01	10.93	0.08	91.09	2.69	30.24	0.90
11X-1, 120–121	151.605	10.90	10.85	0.04	90.42	2.33	24.31	0.42
11X-1, 125–126	151.655	10.92	10.89	0.03	90.76	2.40	25.97	0.32
11X-1, 130–131	151.705	10.58	10.54	0.05	87.80	3.40	27.85	0.41
11X-1, 135–136	151.755	10.75	10.69	0.05	89.11	2.97	27.26	0.46
11X-1, 140–141	151.805	10.72	10.70	0.02	89.14	3.50	32.23	0.18
11X-2, 0–1	151.905	10.70	10.62	0.08	88.53	3.58	31.17	0.70
11X-2, 5–6	151.955	10.37	10.35	0.02	86.25	3.40	24.73	0.15
11X-2, 8–9*	151.985	6.37	6.24	0.13	50.96	10.07	20.60	0.26
11X-2, 10–11	152.005	8.42	8.40	0.02	69.98	9.18	30.58	0.07
11X-2, 12–13*	152.025	9.89	9.69	0.20	80.81	4.60	23.97	1.04
11X-2, 15–16	152.055	10.15	10.11	0.04	84.28	4.45	28.32	0.25
11X-2, 20–21	152.105	10.32	10.30	0.03	85.82	3.40	23.98	0.21
11X-2, 25–26	152.155	10.60	10.49	0.11	87.41	3.40	27.01	0.87
11X-2, 30–31	152.205	10.84	10.82	0.02	90.14	2.61	26.50	0.20
11X-2, 132–133	152.225	10.47	10.44	0.03	87.01	2.35	18.11	0.23
11X-2, 35–36	152.255	10.79	10.74	0.05	89.48	3.30	31.37	0.48
11X-2, 38–39	152.285	10.52	10.46	0.06	87.16	3.50	27.26	0.47
11X-2, 40–41	152.305	10.58	10.49	0.09	87.38	4.08	32.31	0.71
11X-2, 42–43	152.325	10.43	10.37	0.05	86.44	4.40	32.47	0.37
11X-2, 45–46	152.355	10.74	10.69	0.05	89.12	3.28	30.12	0.46
11X-2, 48–49	152.385	10.43	10.41	0.02	86.73	3.43	25.86	0.15
11X-2, 50–51*	152.405	9.65	9.53	0.12	79.47	5.41	26.30	0.58
11X-2, 52–53*	152.425	9.11	8.98	0.13	74.92	5.00	19.93	0.51
11X-2, 55–56*	152.455	8.10	8.00	0.10	66.72	8.20	24.60	0.30
11X-2, 58–59	152.485	10.24	10.19	0.06	84.88	4.50	29.79	0.40
11X-2, 60–61	152.505	10.08	10.04	0.04	83.68	5.99	36.70	0.25
11X-2, 68–69*	152.585	9.87	9.76	0.11	81.38	4.60	24.70	0.60
11X-2, 70–71*	152.605	10.16	9.62	0.54	80.24	4.40	22.27	2.73
11X-2, 72–73	152.625	10.26	10.23	0.03	85.27	3.64	24.69	0.20
11X-2, 75–76	152.655	10.05	10.03	0.02	83.57	4.12	25.10	0.12
11X-2, 78–79	152.685	10.30	10.28	0.02	85.64	3.47	24.17	0.14
11X-2, 80–81	152.705	10.31	10.26	0.05	85.64	3.88	27.01	0.35
11X-2, 83–84	152.735	10.58	10.52	0.05	87.68	2.67	21.64	0.41
11X-2, 85–86	152.755	10.59	10.53	0.06	87.77	2.61	21.35	0.49
11X-2, 88–89	152.785	10.10	10.06	0.04	83.83	3.70	22.88	0.25
11X-2, 90–91	152.805	10.53	10.51	0.03	87.54	3.22	25.88	0.24
11X-2, 93–94	152.835	7.98	7.92	0.06	66.02	8.83	25.99	0.18
11X-2, 95–96	152.855	9.27	9.24	0.03	77.00	5.81	25.28	0.13
11X-2, 100–101	152.905	8.23	8.21	0.02	68.43	7.77	24.61	0.06
11X-2, 102–103	152.925	10.37	10.31	0.06	85.91	3.08	21.84	0.43
11X-2, 105–106	152.955	10.54	10.51	0.03	87.57	2.92	23.51	0.24
11X-2, 99–100	152.985	8.80	8.78	0.03	73.15	5.45	20.29	0.11

Table T1 (continued).

Core, section, interval (cm)	Average mcd	Average carbon (wt%)				Average SiO_2 (wt%)	Carbonate-free elements (wt%)	
		Total	Inorganic	Organic	$CaCO_3$		SiO_2	Organic carbon
11X-2, 110–111	153.005	10.43	10.40	0.03	86.69	3.16	23.76	0.23
11X-2, 115–116	153.055	10.54	10.51	0.03	87.58	3.40	27.38	0.24
11X-2, 118–119	153.085	5.92	5.89	0.03	49.06	15.05	29.54	0.06
11X-2, 125–126	153.155	10.04	9.98	0.06	83.13	4.37	25.92	0.36
11X-2, 128–129	153.185	10.23	10.20	0.02	85.02	2.74	18.27	0.13
11X-2, 130–131	153.205	10.20	10.17	0.04	84.72	3.84	25.15	0.26
11X-2, 135–136*	153.255	9.28	9.18	0.10	76.52	4.30	18.32	0.42
11X-2, 138–139*	153.285	9.58	9.49	0.09	79.06	3.50	16.71	0.44
11X-2, 140–141	153.305	10.26	10.22	0.03	85.20	3.01	20.36	0.20
11X-2, 143–144	153.335	10.41	10.38	0.04	86.46	2.53	18.69	0.30
11X-2, 145–146*	153.355	10.46	10.36	0.10	86.38	3.00	22.03	0.74
11X-3, 0–1	153.405	10.30	10.27	0.04	85.54	3.10	21.44	0.28
11X-3, 5–6	153.455	10.41	10.39	0.02	86.60	3.23	24.11	0.15
11X-3, 10–11	153.505	10.40	10.39	0.01	86.55	2.90	21.56	0.07
11X-3, 15–16	153.555	10.36	10.35	0.01	86.23	3.07	22.28	0.07
11X-3, 20–21	153.605	9.61	9.59	0.02	79.94	4.23	21.09	0.10
11X-3, 25–26	153.655	9.80	9.79	0.01	81.55	3.59	19.47	0.05
11X-3, 30–31	153.705	10.06	10.04	0.01	83.70	3.80	23.33	0.06
11X-3, 35–36	153.755	10.19	10.18	0.02	84.83	3.65	24.07	0.10
11X-3, 40–41	153.805	10.21	10.19	0.02	84.89	3.60	23.82	0.13
11X-3, 45–46	153.855	9.93	9.90	0.03	82.47	4.04	23.07	0.17
11X-3, 50–51	153.905	8.94	8.92	0.02	74.37	6.24	24.34	0.07
11X-3, 52–53	153.925	6.14	6.12	0.02	51.00	13.55	27.65	0.05
11X-3, 54–55	153.945	5.98	5.96	0.02	49.67	12.58	24.99	0.04
11X-3, 56–57	153.965	6.20	6.16	0.04	51.35	12.30	25.29	0.08
11X-3, 58–59	153.985	6.82	6.80	0.02	56.67	9.50	21.92	0.05
11X-3, 60–61	154.005	1.01	0.98	0.03	8.17	29.72	32.36	0.04
11X-3, 62–63	154.025	0.40	0.37	0.02	3.12	25.90	26.74	0.02
11X-3, 64–65	154.045	0.65	0.63	0.02	5.22	24.88	26.26	0.03
11X-3, 66–67	154.065	0.25	0.23	0.02	1.94	28.72	29.29	0.02
11X-3, 68–69	154.085	0.61	0.59	0.02	4.89	25.25	26.55	0.02
11X-3, 70–71	154.105	0.60	0.58	0.03	4.80	22.60	24.05	0.03
11X-3, 72–73	154.125	0.32	0.28	0.03	2.37	23.48	24.05	0.03
11X-3, 74–75	154.145	0.16	0.13	0.03	1.06	25.64	25.92	0.03
11X-3, 76–77*	154.165	0.34	0.32	0.02	2.64	34.60	35.59	0.02
11X-3, 78–79	154.185	0.28	0.25	0.03	2.09	27.72	28.31	0.03
11X-3, 80–81	154.205	0.23	0.20	0.03	1.66	28.00	28.47	0.03
11X-3, 82–83	154.225	0.41	0.37	0.03	3.11	27.77	28.66	0.03
11X-3, 84–85	154.245	0.20	0.14	0.06	1.14	27.51	27.83	0.06
11X-3, 86–87	154.265	0.19	0.16	0.02	1.37	26.22	26.58	0.02
11X-3, 88–89	154.285	1.65	1.62	0.04	13.49	22.95	26.53	0.04
11X-3, 90–91	154.305	4.02	3.99	0.03	33.25	18.58	27.84	0.05
11X-3, 92–93	154.325	4.64	4.62	0.02	38.47	16.20	26.33	0.04
11X-3, 94–95	154.345	5.20	5.18	0.02	43.14	15.42	27.12	0.04
11X-3, 96–97	154.365	4.85	4.83	0.02	40.24	17.20	28.78	0.04
11X-3, 98–99	154.385	4.20	4.18	0.03	34.81	18.11	27.78	0.04
11X-3, 105–106	154.455	4.66	4.63	0.03	38.57	16.75	27.26	0.05
11X-3, 110–111	154.505	7.09	7.06	0.03	58.85	10.20	24.78	0.07
11X-3, 115–116	154.555	7.92	7.90	0.02	65.83	8.83	25.84	0.07
11X-3, 120–121	154.605	7.74	7.72	0.02	64.33	9.29	26.04	0.07
11X-3, 125–126	154.655	8.74	8.72	0.02	72.65	7.22	26.39	0.08
11X-3, 130–131	154.705	8.94	8.93	0.02	74.38	7.23	28.23	0.08
11X-3, 135–136	154.755	7.37	7.35	0.02	61.23	10.68	27.55	0.06
11X-3, 140–141*	154.805	5.88	5.77	0.11	48.14	14.50	27.96	0.21
11X-CC, 2–3	154.885	5.77	5.68	0.09	47.33	17.02	32.31	0.17
11X-CC, 7–8	154.935	5.91	5.88	0.03	49.02	11.30	22.17	0.06
11X-CC, 11–12	154.975	4.85	4.82	0.03	40.17	12.54	20.96	0.05
11X-CC, 18–19	155.045	5.52	5.46	0.06	45.52	11.84	21.73	0.12
12X-1, 0–1*	155.405	3.95	3.85	0.10	32.15	16.20	23.88	0.14
12X-1, 5–6	155.455	4.79	4.73	0.06	39.40	10.63	17.54	0.10
12X-1, 10–11*	155.505	5.02	4.89	0.13	40.78	11.20	18.91	0.22
12X-1, 15–16	155.555	4.43	4.40	0.04	36.66	11.68	18.44	0.06
12X-1, 20–21	155.605	2.63	2.57	0.05	21.43	13.50	17.18	0.07
12X-1, 25–26	155.655	2.31	2.24	0.06	18.70	14.49	17.83	0.08
12X-1, 30–31	155.705	1.77	1.72	0.05	14.35	14.80	17.28	0.06
12X-1, 35–36	155.755	3.72	3.66	0.06	30.48	12.82	18.44	0.09
12X-1, 40–41	155.805	5.23	5.19	0.04	43.23	10.57	18.62	0.07

Table T1 (continued).

Core, section, interval (cm)	Average mcd	Average carbon (wt%)				Average SiO_2 (wt%)	Carbonate-free elements (wt%)	
		Total	Inorganic	Organic	$CaCO_3$		SiO_2	Organic carbon
12X-1, 45–46	155.855	4.41	4.37	0.04	36.42	11.45	18.01	0.07
12X-1, 50–51	155.905	3.32	3.26	0.06	27.18	12.58	17.28	0.08
12X-1, 55–56	155.955	3.11	3.05	0.06	25.42	11.50	15.42	0.08
12X-1, 60–61	156.005	4.08	4.04	0.04	33.67	10.14	15.29	0.06
12X-1, 65–66	156.055	6.04	6.00	0.04	50.00	9.07	18.15	0.08
12X-1, 70–71	156.105	7.49	7.45	0.04	62.06	6.38	16.82	0.10
12X-CC, 0–1	156.515	7.46	7.40	0.06	61.65	5.17	13.47	0.16
12X-CC, 5–6	156.565	9.97	9.92	0.06	82.63	2.90	16.69	0.32

Notes: Opal is not corrected for water. * = adjusted values.